AEDC-TR-75-160

cy 1

ARCHIVE COPY
DO NOT LOAN

APPLICABILITY OF INFRARED SCANNING CAMERAS FOR THERMAL VACUUM TESTING IN THE 12V AND MARK I CHAMBERS

VON KÁRMÁN GAS DYNAMICS FACILITY
ARNOLD ENGINEERING DEVELOPMENT CENTER
AIR FORCE SYSTEMS COMMAND
ARNOLD AIR FORCE STATION, TENNESSEE 37389

December 1975

Final Report for Period July 1, 1973 – June 30, 1975

Approved for public release; distribution unlimited.

AEDC TECHNICAL LIBRARY
5 0720 00033 9103

of U. S. Air Force
AEDC LIBRARY
F40600-75-C-0001

Prepared for

DIRECTORATE OF TECHNOLOGY (DY)
ARNOLD ENGINEERING DEVELOPMENT CENTER
ARNOLD AIR FORCE STATION, TENNESSEE 37389

NOTICES

When U. S. Government drawings specifications, or other data are used for any purpose other than a definitely related Government procurement operation, the Government thereby incurs no responsibility nor any obligation whatsoever, and the fact that the Government may have formulated, furnished, or in any way supplied the said drawings, specifications, or other data, is not to be regarded by implication or otherwise, or in any manner licensing the holder or any other person or corporation, or conveying any rights or permission to manufacture, use, or sell any patented invention that may in any way be related thereto.

Qualified users may obtain copies of this report from the Defense Documentation Center.

References to named commercial products in this report are not to be considered in any sense as an endorsement of the product by the United States Air Force or the Government.

This report has been reviewed by the Information Office (OI) and is releasable to the National Technical Information Service (NTIS). At NTIS, it will be available to the general public, including foreign nations.

APPROVAL STATEMENT

This technical report has been reviewed and is approved for publication.

FOR THE COMMANDER

Marion L. Laster

MARION L. LASTER
Research & Development
Division
Directorate of Technology

Robert O. Dietz

ROBERT O. DIETZ
Director of Technology

REPORT DOCUMENTATION PAGE		READ INSTRUCTIONS BEFORE COMPLETING FORM
1. REPORT NUMBER AEDC-TR-75-160	2. GOVT ACCESSION NO.	3. RECIPIENT'S CATALOG NUMBER
4. TITLE (and Subtitle) APPLICABILITY OF INFRARED SCANNING CAMERAS FOR THERMAL VACUUM TESTING IN THE 12V AND MARK I CHAMBERS		5. TYPE OF REPORT & PERIOD COVERED Final Report-July 1, 1973-June 30, 1975
		6. PERFORMING ORG. REPORT NUMBER
7. AUTHOR(s) J. A. Roux, ARO, Inc.		8. CONTRACT OR GRANT NUMBER(s)
9. PERFORMING ORGANIZATION NAME AND ADDRESS Arnold Engineering Development Center (DY) Arnold Air Force Station, Tennessee 37389		10. PROGRAM ELEMENT, PROJECT, TASK AREA & WORK UNIT NUMBERS Program Element 65807F
11. CONTROLLING OFFICE NAME AND ADDRESS Arnold Engineering Development Center (DYFS) Arnold Air Force Station, TN 37389		12. REPORT DATE December 1975
		13. NUMBER OF PAGES 38
14. MONITORING AGENCY NAME & ADDRESS(if different from Controlling Office)		15. SECURITY CLASS. (of this report) UNCLASSIFIED
		15a. DECLASSIFICATION/DOWNGRADING SCHEDULE N/A

16. DISTRIBUTION STATEMENT (of this Report)

Approved for public release; distribution unlimited.

17. DISTRIBUTION STATEMENT (of the abstract entered in Block 20, if different from Report)

1. Infrared scanning cameras.

18. SUPPLEMENTARY NOTES

Available in DDC

19. KEY WORDS (Continue on reverse side if necessary and identify by block number)

test methods
2 cameras (infrared scanning)
vacuum (thermal)
detection
maps (temperature)
background noise
wavelengths

20. ABSTRACT (Continue on reverse side if necessary and identify by block number)

The results of a study defining the applicability of infrared scanning cameras for thermal vacuum testing in the Aerospace Chamber (12V) and the Aerospace Environmental Chamber (Mark I) are presented. The infrared (IR) cameras were studied as an alternative or complement to the use of thermocouples for detecting test model hotspots or temperature maps. The infrared background

DD FORM 1473, 1 JAN 73 EDITION OF 1 NOV 65 IS OBSOLETE

20. ABSTRACT (Continued)

noise sources of the chambers are defined along with their impact upon the cameras' performance and temperature-measuring accuracy. The infrared cameras are shown to be compatible with the SDS 9300 computer for digitizing and storing the camera data.

AFSC
Arnold AFS Tenn

PREFACE

The work reported herein was conducted by the Arnold Engineering Development Center (AEDC), Air Force Systems Command (AFSC), under Program Element 65807F. The results of the research were obtained by ARO, Inc. (a subsidiary of Sverdrup & Parcel and Associates, Inc.), contract operator of AEDC, AFSC, Arnold Air Force Station, Tennessee. The work was performed under ARO Project Numbers VF470 and V35S-62A. The author of this report was J. A. Roux, ARO, Inc. The manuscript (ARO Control No. ARO-VKF-TR-75-94) was submitted for publication on June 26, 1975.

CONTENTS

ILLUSTRATIONS

TABLES

APPENDIXES

1.0 INTRODUCTION

In ground test facilities, it is desirable to economically collect the optimum amount of quantitative and qualitative data without interferring with the test article. For thermal vacuum testing, this presents some unique problems. To determine the temperature at points of interest it is presently necessary to employ thermocouples. This has the disadvantage in that the thermocouples cannot be used at just any arbitrary location on the test article because of installation problems. In addition, since orbiting vehicles are spin stabilized, the testing of rotating apparatus is difficult due to the twisting of the thermocouple wires. For some tests, the thermocouple wires even cause substantial cooling losses. Finally, the use of thermocouples limits the determination of the surface temperature of a test vehicle to the discrete points where the thermocouples are located. Many of the disadvantages associated with the thermocouples could be eliminated by utilization of the infrared (IR) scanning camera.

The IR camera is already being used in aerodynamic heating test applications (Refs. 1 and 2); the heat-transfer coefficient is determined through recording the transient temperature response of the wind tunnel model. At present, the IR camera can be used to determine the blackbody surface temperature of test articles in the range of -30°C to 850°C with an InSb detector (2 to 5 μ) or -50°C to 850°C with a mercury-cadmium-telluride detector (HgCdTe) (8 to 14μ). In addition, the surface temperature of many points within the camera's field of view can be determined, and not just at a few discrete locations as with thermocouples. The IR camera could be very beneficial in quantitatively and qualitatively defining test vehicle hotspots (trouble spots). Also, surface temperatures of rotating test apparatus could be determined without concern over the twisting of thermocouple wires.

The IR camera is particularly attractive as a test instrument because it senses the natural infrared radiation emitted by surfaces in the 2- to 5-μ or 8- to 14-μ wavelength bands (depending upon which detector is used). Thus, the detection of this naturally emitted radiation does not interfere with the test model in any manner. This method of data acquisition requires no physical contact between the test object and the data recording instrument. At present, the temperature resolution of the IR camera is very much less than 1°C, which is as good or better than the thermocouple. The IR camera can also be used to determine the transient temperature response of test articles due to its very high

frame speed. This instrument also appears to have excellent potential for coupling its application with a computer to record and analyze large amounts of test data quickly and accurately.

Many scientific, test-orientated organizations already have and are using the IR scanning camera. At the Institut fur Raumsimulation of DFVLR in West Germany the IR scanning camera is presently being used to locate model hotspots (Ref. 3). Also, at the European Space Research Organization (ESTEC), Noorswijk, Holland, where the largest space-simulation chamber in Europe is installed -- having a diameter in the test plane of three meters -- the IR scanning camera is in use. Applications of the IR scanning camera there include the determining of the surface temperature of a satellite in the space-simulation chamber.

2.0 CAMERA FUNDAMENTALS OF OPERATION

In this section the basic principles of camera operation will be given for IR scanning cameras from three manufacturers: AGA, DYNARAD, and Barnes. Descriptions of these three cameras are included to provide a representative cross section of available IR scanning cameras. The AGA Model 680 was used primarily for this study since it was readily available; however, the purpose of this study and the results obtained pertain to applicability of the general category described as IR scanning cameras for thermal vacuum testing. The AGA Thermovision® Model 680 is the scanning camera which has been purchased by the von Kármán Gas Dynamics Facility (VKF) for the purposes of acquiring aerodynamic heating data on wind tunnel models. The AGA Thermovision IR scanning camera operates on the principles depicted in Fig. 1a. The camera picks up the IR radiation emitted by a body and focuses it on a detector that converts it to an electrical signal. The detector that will be required (as shown later) for thermal vacuum purposes is the photoconductive HgCdTe (8 to 14 μ) which requires cooling by liquid nitrogen (LN_2). The primary optics of the camera (camera lens) form an image of the object in a plane situated inside the vertical scanning prism. The image is scanned vertically by rotation of the prism about its horizontal axis. This results in a horizontal, virtual line-image being formed within the second scanning prism. The line-image is then scanned horizontally in turn by rotation of the second prism about its vertical axis. Both prisms are eight-sided. The horizontal scanning prism is flat in form and rotates about its short axis at a speed of 12,000 rpm. The prism is mounted together with a position pick-off ring on a single flange coupled directly to the shaft of the horizontal-drive motor. The vertical scanning prism is drum-shaped. It rotates at right angles to the horizontal prism, scanning the image approximately once vertically for every 70 horizontal scans.

The operation of the rotating prisms is depicted in Fig. 1b. In position 1, radiation from point 1 in the image will reach the detector. When the prism is in position 2, the detector will look at point 2 situated medially in the image. Thus, the prism will have the same function as if the detector element were moved quickly along the line 1, 2, 3. For each revolution of the prism, eight lines are scanned, and, as the prism makes 200 rev/sec, 1,600 lines are scanned per second.

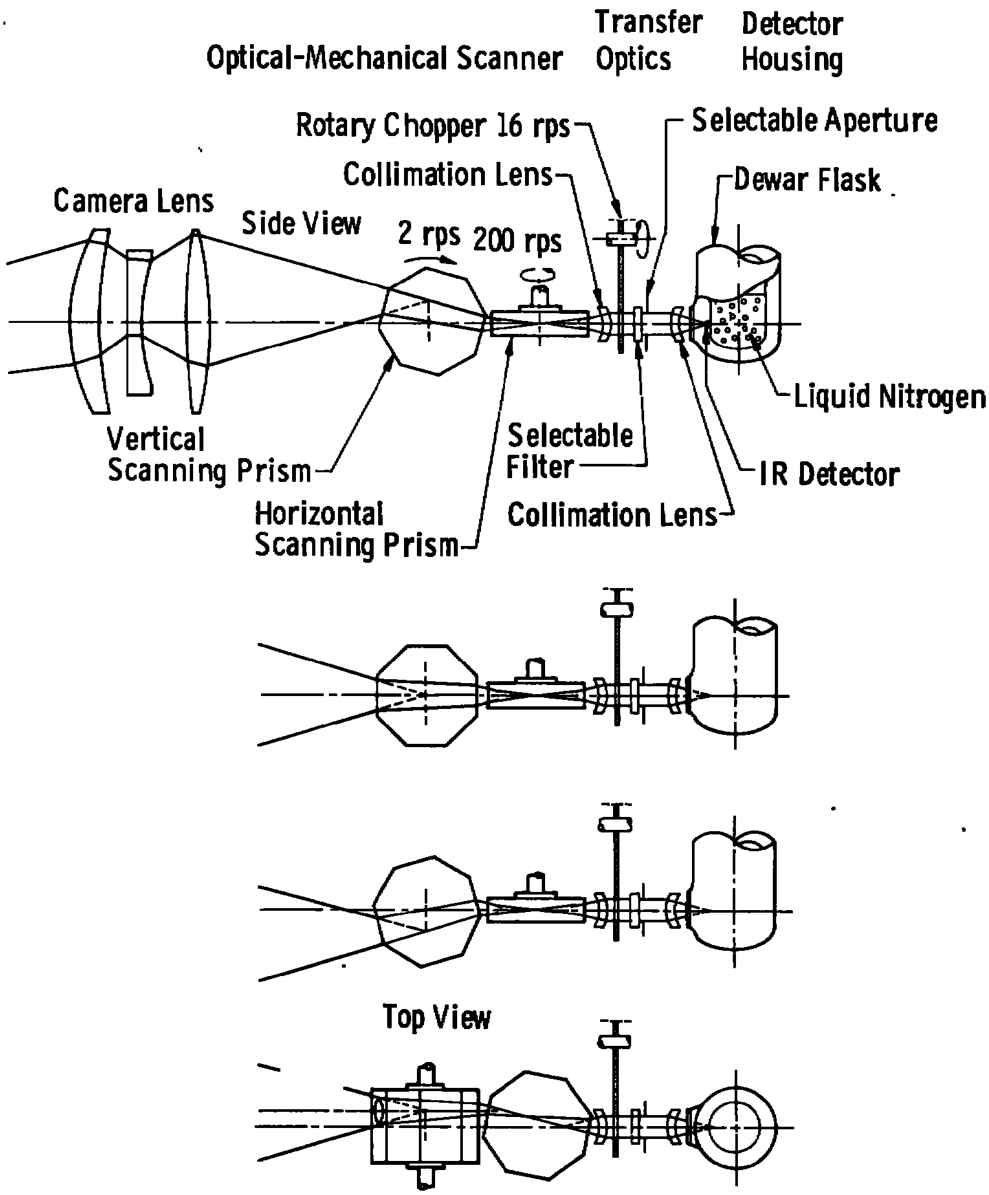

a. Scanning principles

Figure 1. Operation fundamentals of the AGA Model 680® IR scanning camera.

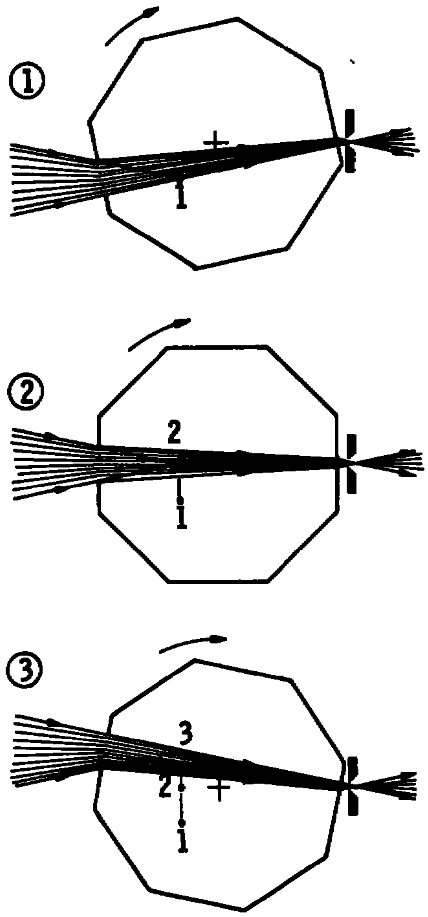

b. Operation of rotating prisms
Figure 1. Concluded.

The detector signal is amplified and fed to the display unit (or computer), where it is processed and used to modulate the intensity of the beam in the picture (or is digitized and stored in the computer along with the vertical and horizontal sync signals). The beam sweeps across the tube face in a pattern corresponding to the scanning pattern of the camera.

The thermal picture on the screen is taken at 16 frames/sec. The camera can be focused remotely from the display unit. The size of the picture on the tube is 50 mm by 60 mm. Temperature differences of less than 0.2°C can be distinguished on objects at approximately room temperature. The spatial resolution is about 100 picture elements per line but can be increased by a factor of three before the optical system limits itself. The range of detectable blackbody temperatures is -50°C to 850°C for an HgCdTe detector (8 to 14 μ).

The number of lines per picture (frame) is nominally 100. By proper choice of the ratio between the horizontal and vertical scanning frequencies, the line raster will move slowly in the vertical direction, and a photo of the screen taken with an exposure time of 0.5 sec or longer will contain so many superimposed frames that the line pattern is hardly noticeable. The instantaneous field of view of the camera is quoted as 3.5 mrad for a 45-deg by 45-deg field of view lens. Shown in Appendix A are charts with detailed lens information (focal length, depth of field, etc.) for three lenses: 10-deg by 10-deg, 25-deg by 25-deg, and 45-deg by 45-deg fields of view lens.

Shown in Fig. 2 is a sketch depicting the basic operating principles of the DYNARAD® camera (Model 810). Infrared radiation enters the aperture at the front and impinges upon a dichoric which reflects the

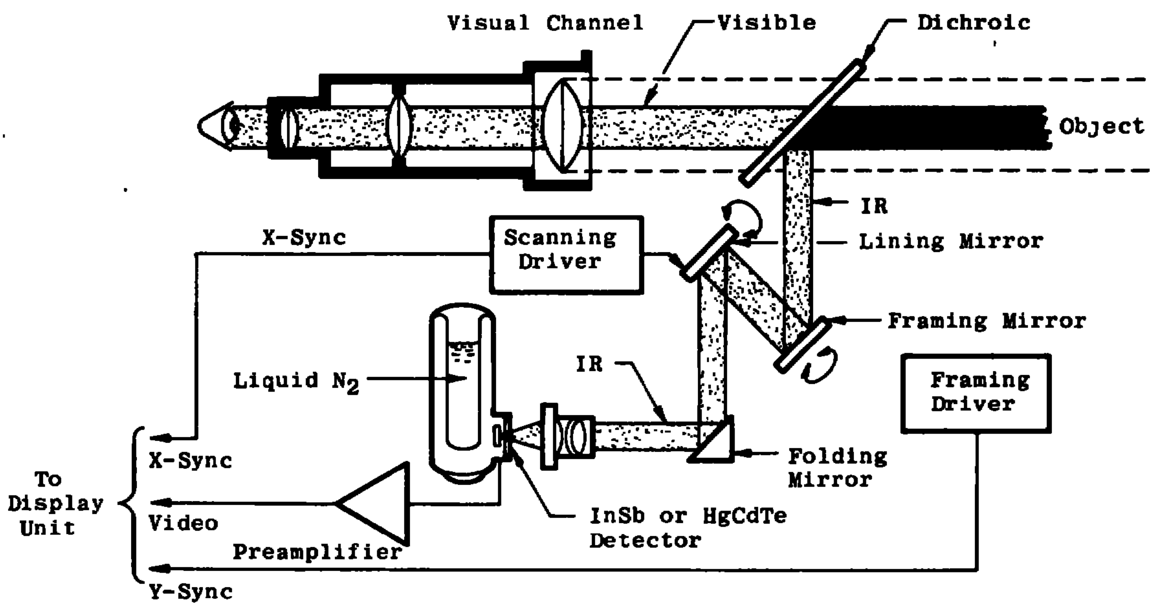

Figure 2. Operation fundamentals of the DYNARAD Model 810® IR scanning camera.

infrared radiation downward and transmits the visible radiation to a spotting scope. The IR radiation proceeds from the dichoric to a first-surface framing mirror. From the framing mirror, the beam proceeds upward to the line-generating mirror whose axis of rotation is orthogonal to that of the framing mirror. Redirected downward again by the lining mirror, the beam strikes a folding mirror and is directed to the infrared transmissive lens and thence focused on the detector located behind a window in a dewar containing liquid nitrogen. The detector signal is then fed to the CRT (or computer) with frame and line scan synchronization

from the camera. The camera is normally furnished with an indium antimonide detector sensitive from 2.0 to 5.4 micrometers, which corresponds to a region of relatively good atmospheric transmission of infrared radiation. An HgCdTe detector, which operates in another major atmospheric window region between 8 and 14 micrometers is also available and would be most applicable for AEDC vacuum chamber use.

Targets near room temperature radiate most strongly in the 8- to 14-μ band. Approximately 40 percent of total ambient temperature emission occurs in this band. The range of detectable blackbody temperatures is -20°C to 500°C. The focus is motor driven and controlled from the front panel of the control and display unit. The total field of view is variable in 5-deg steps from 10 to 35 deg. Instantaneous field of view is quoted as 1.7 mrad giving a 200-resolution element picture at 10-deg by 10-deg field of view and a maximum 400-element picture at 20-deg field of view. A large optical aperture with a d-c coupled HgCdTe detector results in a minimum resolvable temperature difference of 0.05°C with frame times of 1 to 16 sec. The scanning rate is 60 lines/second with resultant thermal pictures of 50 to 800 lines depending on the frame rate. Both horizontal and vertical scanning are linear and unidirectional.

The basic principles of operation of the Barnes® IR scanning camera are shown in Fig. 3. In operation, the Model 101 scans its target in two dimensions, vertical and horizontal. This scanning is accomplished

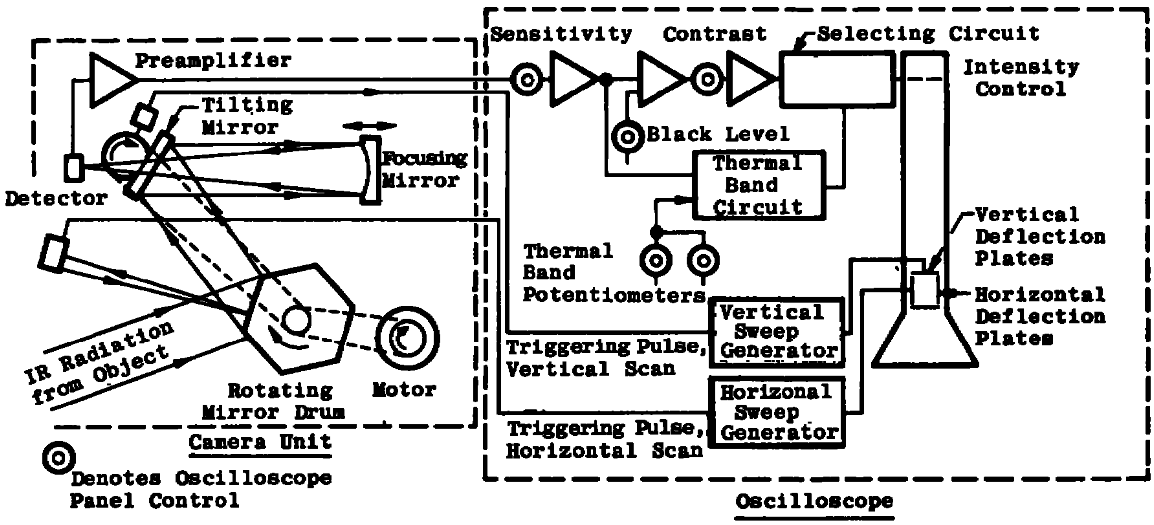

Figure 3. Operation fundamentals of the Barnes Model 101® IR scanning camera.

horizontally by means of a high-speed, six-sided, mirrored drum that rotates at 4,500 rpm. The IR radiation entering the camera is reflected from the horizontal drum and strikes a rocking, vertical scan mirror. It is then collected by a concave mirror which, in turn, focuses the energy on a small, highly sensitive detector. The detector's output is an electrical signal that is directly proportional to the amount of radiation impinging upon it. This signal is amplified, processed, and displayed on a cathode ray tube as an intensity-modulated raster -- a thermal image of its target.

For applications involving CO_2 (10.6 μ) laser studies, low temperature targets and/or long atmospheric paths, a cooled lead-tin-telluride detector is optionally available. This trimetal detector provides excellent sensitivity throughout the 8-μ to 12-μ region. It is packaged in a dewar with an LN_2 hold time of four hours. The detectable temperature range of this camera is -20°C to 150°C.

It should be mentioned that none of the above described cameras can be used in vacuum. Thus, it will be necessary to use the IR scanning camera outside the vacuum chamber and obtain data through a chamber viewport. It will be necessary that the viewport window have a high transmissivity and a low emittance.

In the preceding discussion, the spatial resolutions of the various cameras were presented. To more clearly demonstrate spatial resolution, Fig. 4 has been included; this figure depicts how spatial resolution

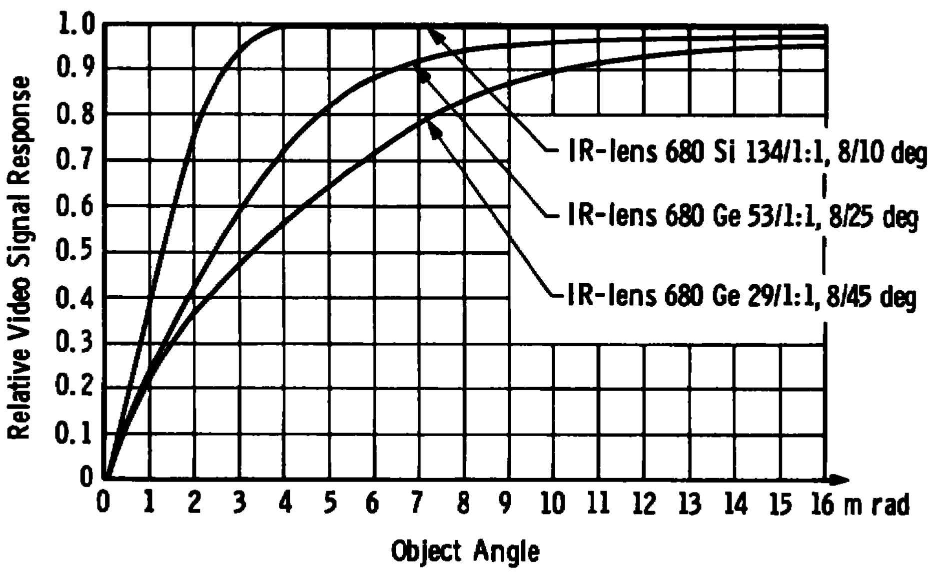

Figure 4. Spatial resolution for the AGA Model 680® IR scanning camera, Ref. 5.

is defined for the AGA Model 680 camera (Ref. 4). Three curves are shown corresponding to three field-of-view lenses: 10-deg, 25-deg, and 45-deg fields of view (Appendix A). The spatial resolution for this camera is defined on the basis that the size of a slit (acting as an aperture to a blackbody source) is reduced such that the modulation drops to 50 percent. For example, in Fig. 4 the spatial resolution for the 25-deg field-of-view lens is 2.5 mrad. However, in order to measure temperature it appears that the spatial resolution must be defined as the smallest slit opening which will still yield 100-percent modulation; hence, the spatial resolution for temperature measurement would be about 10 mrad for the 25-deg field-of-view lens.

3.0 CHAMBER DESCRIPTION

3.1 BACKGROUND

The IR camera would be most useful in its application to testing performed in two AEDC vacuum chambers. These chambers are the Aerospace Chamber (12V) which is 12 ft in diameter and 35 ft high and the Aerospace Environmental Chamber (Mark I) which is 42 ft in diameter and 82 ft high. Hence, it is desirable to define the sources of IR noise associated with these chambers. It should be remembered that ideally the IR camera would only respond to the IR radiation emitted by the test vehicle. However, IR radiation from other sources will be incident upon the test apparatus and will be reflected. The IR scanning camera cannot distinguish between the IR radiation emitted by the test vehicle and the IR radiation reflected from the test vehicle; it will respond to the sum of these two signals. Thus, it is necessary to investigate the sources of IR noise in both the 12V and Mark I chambers, to determine their magnitude, and how they will affect the camera performance. Also, it is desirable to recommend techniques for either eliminating or minimizing the chamber IR noise. The chamber IR noise will also have to be considered in the camera calibration.

Before presenting a detailed discussion of the chamber IR noise sources, it is instructive to observe in Fig. 5 some typical test vehicle surface temperatures. For convenience, the test object geometry is chosen as a sphere. Figure 5 shows the temperature distribution about a sphere with an incident radiative flux of one solar constant and for three different surface finishes: polished aluminum, white paint, and black paint. The solid curves depict the temperature distribution for a nonthermally conducting sphere. The line labeled T_s corresponds to a sphere with infinite thermal conduction. The other two curves

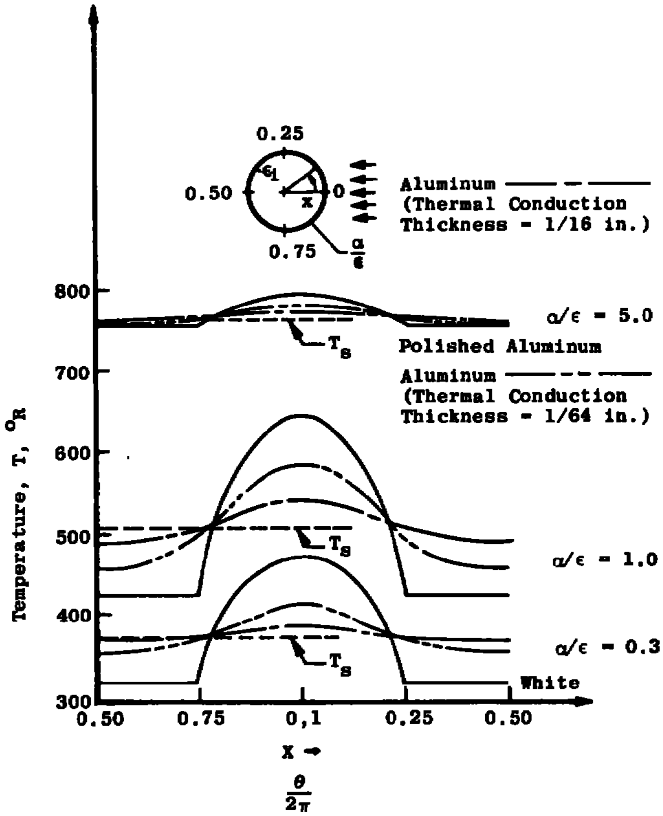

	Surface Coating		
	Black	White	Polished Aluminum
α	1.00	0.27	0.25
ϵ	1.00	0.90	0.05
ϵ_i	1.00	1.00	1.00
T_k, °R	144	144	144
T_s, °R	511.6	380.0	764.1

Black Sphere
AEDC-TR-72-54

T_s = 513°R ($T_k \approx$ 144°R)

T_s = 515°R (No Shroud)

Figure 5. Typical test sphere surface temperature distributions.

correspond to thermally conducting spheres of different wall thicknesses. If the sphere is rotating, then the temperatures would even more closely approach T_S. It should be noted that if electronic equipment (heat generating or power dissipating) were in operation onboard the sphere, then the temperatures shown in Fig. 5 would be higher.

It might be well to note here that when power dissipating equipment is onboard a space vehicle, local hotspots may be created. This is where the IR camera would be of extreme value, since it can especially detect higher temperatures. For initial use, the IR camera could be useful for detecting the location of hotspots on models. Viewing the test object with the IR camera would then help to pinpoint locations where thermocouples should be placed in order to more clearly define the temperature in the vicinity of the hotspot. Presently, since thermocouples cannot be placed everywhere, it is possible that a piece of hardware could be tested without locating the hotspots which would indicate faulty fabrication (insulation) or the overheating or malfunction of onboard electronics. As an initial use of the IR camera it would be possible to at least locate these problems areas and then a more detailed investigation could be performed

with thermocouples. Ultimately, the IR camera would be used to quantitatively and qualitatively determine the locations and temperature levels of the hotspots and the entire test vehicle.

3.2 12V CHAMBER DESCRIPTION

A sketch of the 12V thermal vacuum chamber is shown in Fig. 6. The chamber walls are lined with a liquid-nitrogen-cooled liner. Also, there is a viewport in the test section of the chamber. Since an IR camera cannot be used in vacuum, the camera must be mounted outside the chamber and view the test article through the port. The solar simulator (Ref. 5) used to irradiate the test article is an off-axis system consisting of three basic components: a source lamp array, an optical integrating lens system, and a collimating mirror. The source is an array of seven 20-kw xenon arc lamps in elliptical reflectors. The radiation from the lamps passes through a quartz integrating lens unit

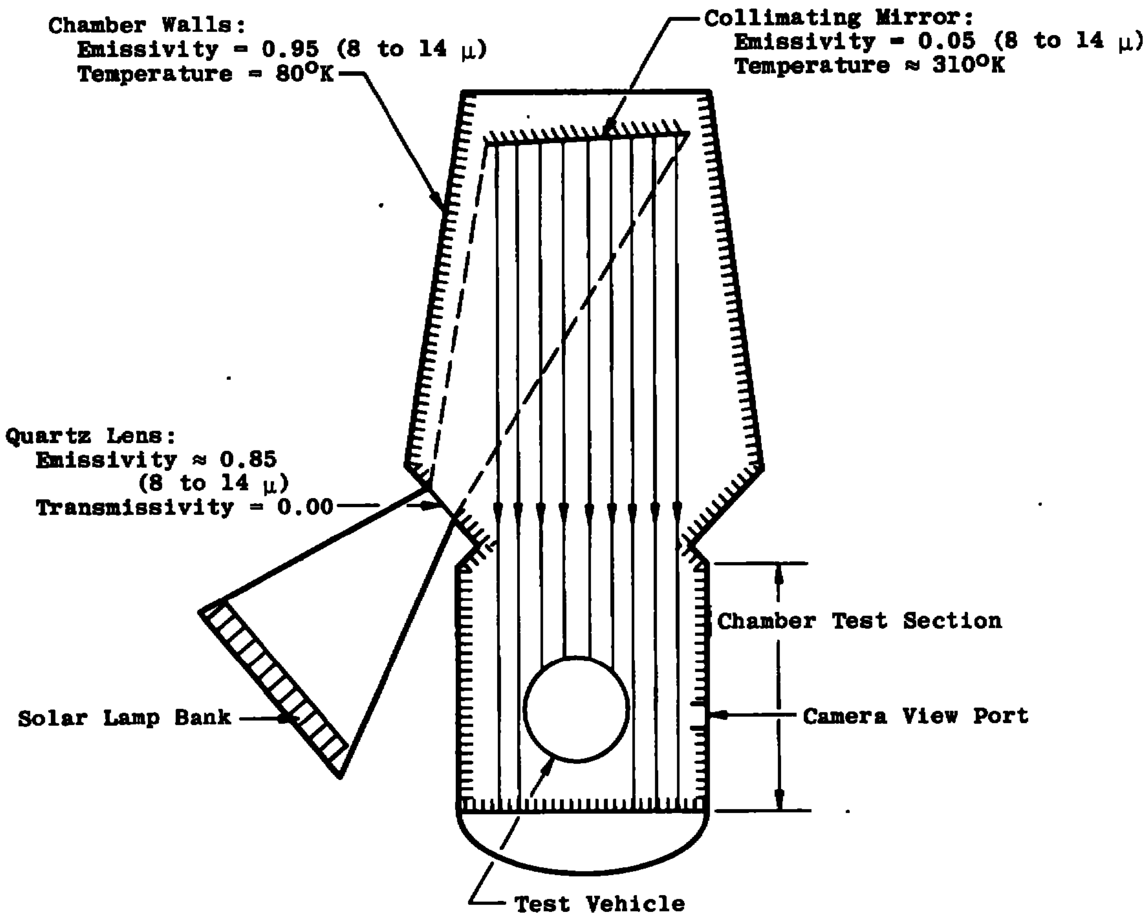

Figure 6. Sketch of 12V chamber.

in the chamber wall to a 10-ft-diam aluminized collimating mirror. The mirror directs a collimated beam down into the test volume. Transmittance and reflectance properties of quartz are shown in Fig. 7; the solid curve corresponds to the quartz reflectance, and the dashed curve corresponds to the quartz transmittance. Since the quartz will transmit radiation up to about 3.5 μ, the xenon lamps will act as a high IR noise source below 3.5 μ. In order to avoid the lamps as a noise source it is necessary to use an HgCdTe detector which responds in the 8- to 14-μ region. Figure 7 shows the quartz lens to be opaque in this wavelength region, thus blocking any IR noise (8 to 14 μ) from the xenon lamps from entering the chamber. The two significant sources of IR chamber noise (8 to 14 μ) associated with the 12V chamber are the collimating mirror and the quartz integrating lens. The collimating mirror has an emissivity of about 0.05 (8 to 14 μ), and the quartz lens has an emissivity of about 0.65 (310°K) (8 to 14 μ). These sources of IR noise (8 to 14 μ) become more intense as the temperature of the mirror and lens increases. The significance of these IR noise sources also depends upon the test vehicle surface temperature and emissivity. A detailed mathematical description and a parametric analysis of these noise sources will be discussed later. It should be pointed out that for testing with the solar simulator off, the chamber is practically noise free since the integrating lens and collimating mirror become very cold due to radiative cooling.

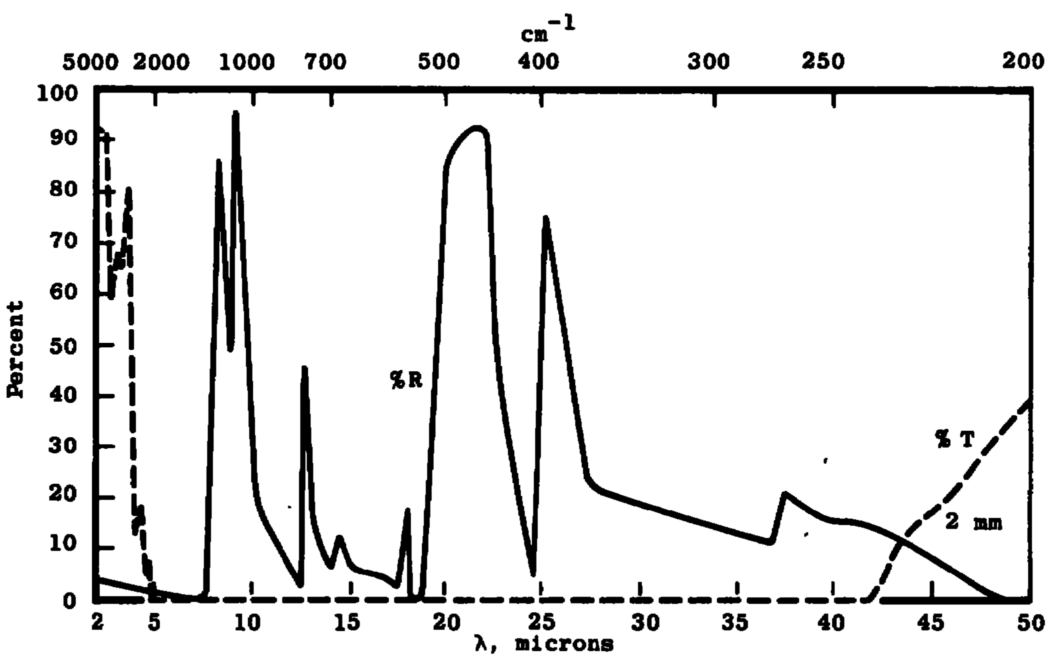

Figure 7. Transmittance and reflectance of quartz, 1 cm thick.

3.3 MARK I CHAMBER DESCRIPTION

A sketch (Ref. 7) depicting the main features of the Mark I chamber is shown in Fig. 8. The chamber is 42 ft in diameter, 82 ft high, and has elliptical heads. The nominal working dimensions of the chamber are 34 ft in diameter and 65 ft in height. To conduct thermal balance tests, the Mark I chamber has an array of 1,000-w quartz envelope-tungsten iodide lamps. The significant point about these lamps is the quartz envelope. As noted in Fig. 7, the quartz will be transparent to

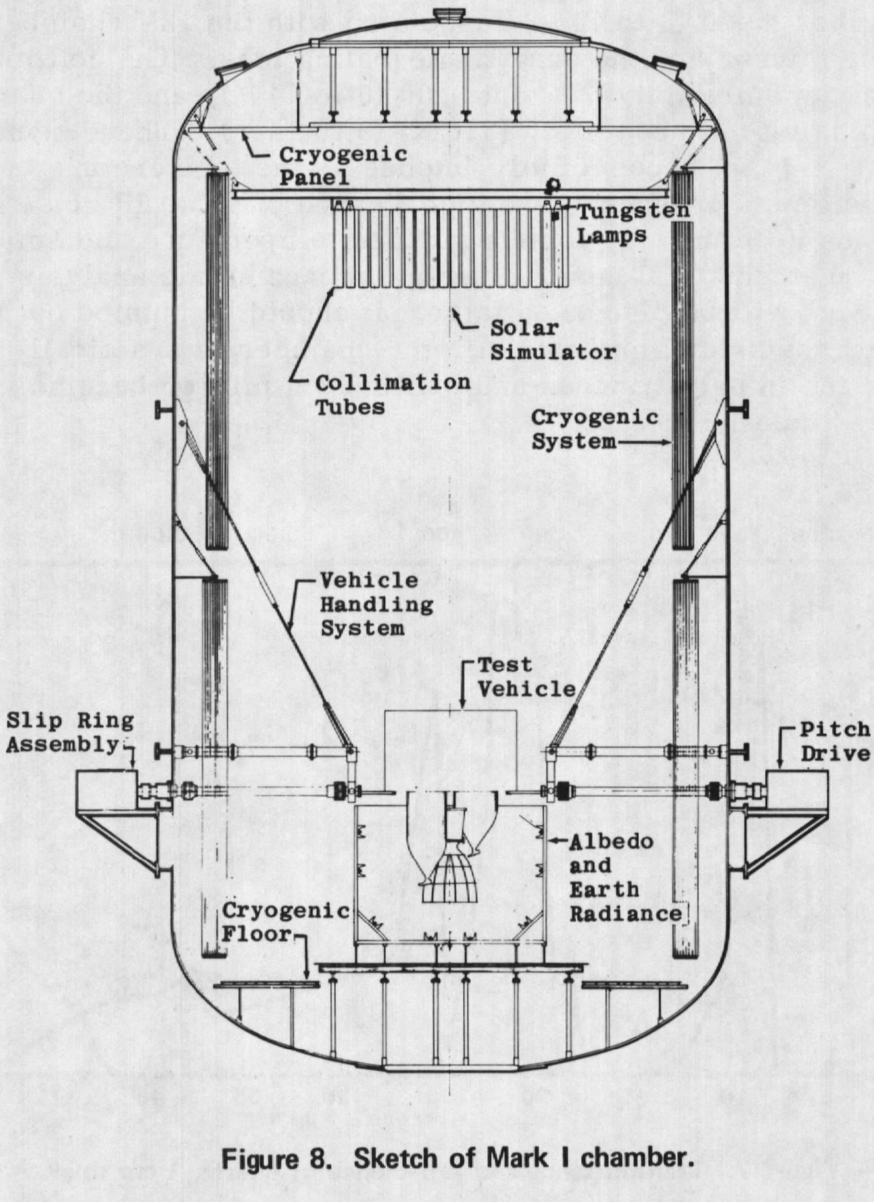

Figure 8. Sketch of Mark I chamber.

almost all of the solar energy. However, it will appear as opaque to radiation in the 8- to 14-μ region and does not allow any IR noise (8 to 14 μ) from the internal portion of the lamp to be present inside the chamber. But the quartz envelope will emit energy in the 8- to 14-μ wavelength region characteristic of the quartz envelope temperature with an emissivity of about 0.65. The emission by these quartz envelopes is a large source of IR noise. The remainder of the Mark I chamber is essentially free of IR noise, since the entire area of the chamber is maintained at liquid-nitrogen temperature. The infrared noise (8 to 14 μ) emitted by the quartz envelopes depends upon the temperature of the envelopes. An exact temperature is not known; however, several hundred degrees Kelvin would be a reasonable temperature.

An IR noise source with such a high temperature would render the Mark I chamber unapplicable for use of the IR scanning camera with the solar simulator in operation. This is because the radiation emitted by the quartz envelope and subsequently reflected from the test article would be much larger than the radiant power emitted by the test article. To determine the temperature of a body, the IR camera must primarily respond to the emitted radiant power from the test article and not to the reflected radiation emitted from the quartz envelopes. The IR camera would still be useful for low reflecting test articles (blackbodies), since the reflected power would be negligible. Also, the IR camera would still be useful for a test not requiring use of the solar simulator. Even when the solar simulator is operating, the IR camera might still provide qualitative information. The quartz envelopes on the tungsten iodide lamps would require cooling in order to usefully employ the IR camera for temperature measurement of nonblack surfaces in the Mark I chamber when the solar simulator is operating.

3.4 ANALYSIS OF 12V AND MARK I CHAMBERS

As pointed out earlier (Section 3.2) the IR scanning camera responds to the radiative power leaving a small area element in its field of view, and the image produced by the camera is the composite of these small area signals. The signals coming from these small areas are composed of two components: radiation emitted by an area element

and radiation which is reflected from an area element. As mentioned, the radiation reflected from an area element originates from two sources (IR noise sources -- 8 to 14 μ): the quartz integrating lens and the aluminized collimating mirror. The IR camera cannot distinguish between the radiative power emitted from the small area element and the radiation reflected from the area element; thus, it is instructive to determine how these IR noise sources affect the camera output for 12V applications.

Assume that the camera was calibrated with the solar simulator not operating and using a blackbody source. The blackbody temperature is varied to determine the corresponding camera analog signal (voltage). Knowing the surface emissivity or reflectivity (8 to 14 μ) of the various paints used on a test vehicle, then the calibration curves can easily be adjusted to account for the fact that the surface emissivity is different from that of a blackbody (unity emissivity). The question now is, what temperature will the camera calibration yield when the camera is used with the solar simulator operating and the camera subjected to the noise signals of the quartz integrating lens and the aluminized collimating mirror. The influence of these noise sources depends on several parameters such as lens temperature, lens emissivity, mirror temperature, mirror emissivity, test apparatus temperature, and test apparatus emissivity. Also, the chamber noise will depend upon whether the test article is a diffuse or specular reflector. The results of selecting realistic values for these parameters are shown in Tables 1 and 2.

No surface is perfectly diffuse or perfectly specular; thus, a real surface will yield results somewhere in between these ideals. Figure 5 may be used to obtain an idea of the temperature level of surfaces of various solar absorptances and IR emissivities. These surface temperatures may, however, be changed (higher or lower) depending upon whether energy absorbing (cryogenic fluids) or energy dissipating (electronics, etc.) equipment are onboard the test vehicle. It should also be pointed out that painted surfaces appear as diffuse surfaces, whereas highly polished surfaces appear as specular surfaces. Presently, the water-cooled collimating mirror in the 12V chamber operates at about 310°K (100°F). The quartz integrating lens temperature is not accurately known; however, by water cooling the flange holding this quartz lens it should be easily cooled to 310°K (100°F). In accordance with Fig. 5, the range of test article surface temperatures has been varied from 250 to 450°K. It was found that the greatest source of IR noise in the 12V chamber is the collimating mirror. The only method to reduce this noise source would be to use some other

Table 1. Temperature Error Caused in 12V Chamber by IR Noise Sources, Diffuse Model

TTV, °K	RTV = 0.95 TL = 310°K TM = 310°K	RTV = 0.75 TL = 310°K TM = 310°K	RTV = 0.65 TL = 310°K TM = 310°K
250	257.12*	251.14*	250.71*
275	280.74*	275.91*	275.56*
300	304.79*	300.76*	300.47
325	329.09*	325.65	325.40
350	353.58*	350.57	350.35
375	378.20*	375.50	375.31
400	402.90*	400.46	400.28
425	427.67*	425.42	425.26
450	452.48*	450.39	450.24

TTV, °K	RTV = 0.45 TL = 310°K TM = 310°K	RTV = 0.25 TL = 310°K TM = 310°K	RTV = 0.05 TL = 310°K TM = 310°K
250	250.31*	250.13	250.02
275	275.25	275.10	275.02
300	300.21	300.08	300.01
325	325.18	325.07	325.01
350	350.15	350.06	350.01
375	375.14	375.06	375.01
400	400.12	400.05	400.01
425	425.11	425.05	425.01
450	450.11	450.04	450.01

*Signal below minimum detectable signal
TTV = True temperature of test vehicle
RTV = Reflectance of test vehicle
TL = Temperature of integrating lens
TM = Temperature of collimating mirror

Table 2. Temperature Error Caused in 12V Chamber by IR Noise Sources, Specular Model

TTV, °K	RTV = 0.95 TL = 310°K TM = 310°K	RTV = 0.75 TL = 310°K TM = 310°K	RTV = 0.65 TL = 310°K TM = 310°K
250	341.89*	269.52*	262.47*
275	355.77*	290.98*	285.14*
300	371.68*	313.46*	308.46
325	389.31*	336.61	332.27
350	408.31*	360.24	356.39
375	428 44*	384.18	380.72
400	449.44*	408.35	405.20
425	471.14*	432.69	429.79
450	493.39*	457.16	454.45

TTV, °K	RTV = 0.45 TL = 310°K TM = 310°K	RTV = 0.25 TL = 310°K TM = 310°K	RTV = 0.05 TL = 310°K TM = 310°K
250	255.68*	252.33	250.37
275	279.56	276.86	275.29
300	303.78	301.54	300.24
325	328.23	326.32	325.21
350	352.83	351.15	350.18
375	377.53	376.03	375.16
400	402.29	400.93	400.15
425	427.11	425.86	425.14
450	451.96	450.08	450.13

*Signal below minimum detectable signal

coolant than water, such as freon. However, this would require additional cost. Because of this, the calculations were performed by assuming the collimating mirror to be only water cooled. An outline of the derivation of the equations used for the results shown in Tables 1 and 2 is presented in Appendix B.

In Table 1 the symbols TTV, RTV, TL, and TM represent the true temperature of the test vehicle, the reflectance of the test vehicle, the temperature of the integrating lens, and the temperature of the collimating mirror, respectively. The values in the table are those which the camera would indicate. For high surface reflectances and low temperatures it is seen that the radiation signal incident upon the camera is below the minimum detectable signal of the camera. However, in the range of detectable radiation levels the camera is seen to yield temperatures within 1°K of the true value. The results in Table 1 are, of course, for a diffuse test article. Here it is seen that for diffusely reflecting objects the IR camera is not limited by IR chamber noise but by the minimum detectable signal.

Table 2 shows the effect of the 12V chamber noise for a specular model. The temperatures which the camera would yield are seen in comparison to the true temperature of the test vehicle. In Table 2 the footnote indicates that for highly reflecting test articles and low temperatures the camera is limited by its minimum detectable signal. When the camera is operating in the range above the minimum detectable temperature it is seen that for RTV = 0.75 the maximum temperature error is about 12°K at TTV = 325°K. If it is required that a maximum error of 5°K be established, then it is seen that the chamber IR noise sources invoke an additional limit on the camera's range of applicability. Figure 9 shows a summary of the results depicted in Tables 1 and 2. Requirements in Fig. 9 are that the maximum temperature error be 5°K. The curve marked diffuse is limited only by the minimum detectable signal of the IR camera. The emittance corresponds to the emittance in the 8- to 14-μ wavelength region. The curve marked specular shows the camera is more significantly affected by IR chamber noise for specular surfaces as opposed to diffuse surfaces. The range of applicability for the diffuse and specular surfaces is the region of Fig. 9 which lies to the right and top of the curves marked diffuse and specular, respectively. Since the IR camera performance for diffuse surfaces is limited only by the IR camera's ability to detect a small signal, the curve marked diffuse is the best that can be expected. The curve marked specular is shifted from the diffuse curve due to chamber IR noise. The specular curve can be made to approach the diffuse curve by reducing the chamber IR

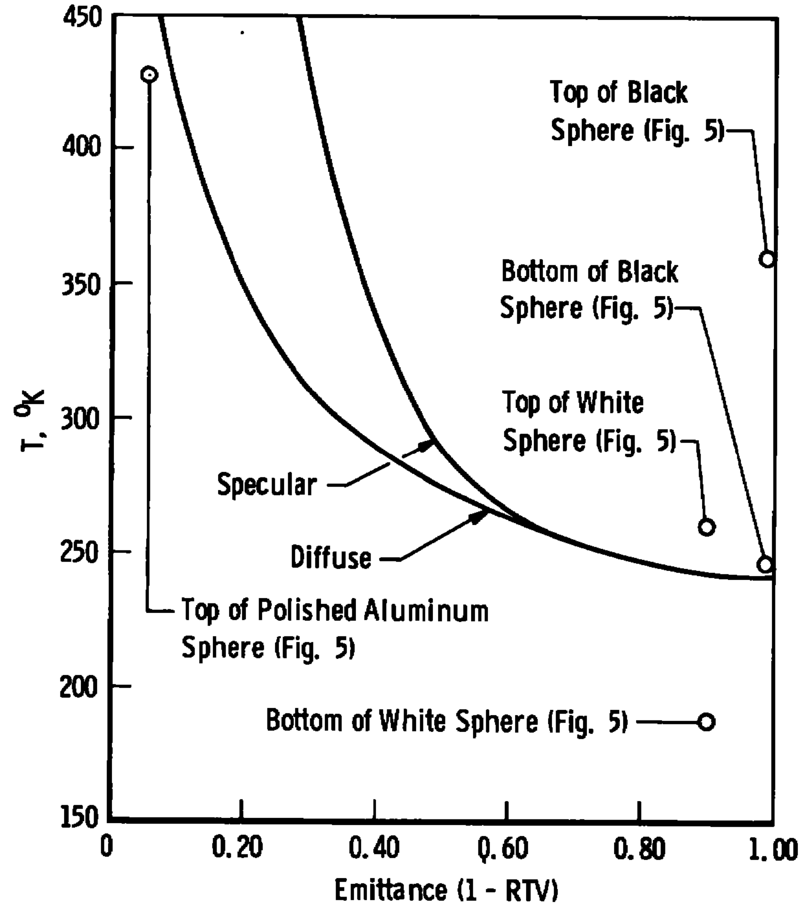

Figure 9. Applicability range of the IR scanning camera in the 12V chamber for 5°K maximum temperature error.

noise. This can be accomplished by cooling the collimating mirror with freon for example and, therefore, reducing the intensity of the noise emanating from the collimating mirror.

The diffuse curve in Fig. 9 is actually valid for temperature measurement within 1°K accuracy as seen from Table 1. It should be pointed out that the specular curve will be shifted to the left if the temperature error requirements are relaxed and will be shifted to the right if the temperature error requirements are tightened. If, however, the maximum temperature error of 5°K is maintained, then from Table 2 it can be seen that the camera can still be useful for detecting hotspots although the absolute value of the temperature measurement will not be within 5°K for a specular surface. For example, if RTV = 0.65 and there is a local hotspot of 325°K in a region surrounded by temperatures of 300°K, the temperature difference would be 25°K. The IR camera would yield temperatures

of 332.27°K and 308.46°K, thus indicating a hotspot having a temperature difference of 23.81°K. Thus, although the temperature measurements would not be with a 5°K tolerance for each spot, the IR camera could still be used to determine the location of hotspots by defining temperature differences. It should also be mentioned that the specular curve in Fig. 9 could also be shifted to the left by using one reference thermocouple in order to correct for the IR chamber noise.

Also shown in Fig. 9 is some of the data from Fig. 5. This shows that determination of the entire temperature range of the black painted sphere could be obtained with the IR camera. Only the measurement of points near the top of the white painted sphere could be measured; the bottom portion of the white sphere is below the minimum detectable signal. The polished aluminum sphere would not be detectable since it is a specular surface and has a very high reflectance in the 8- to 14-μ wavelength region.

Tables 3 and 4 show the effect of the IR noise sources in the Mark I chamber; these tables correspond to the present solar simulator in the Mark I chamber equipped with a water-cooled quartz cover over the end

Table 3. Temperature Error Caused in Mark I Chamber by IR Noise Sources, Diffuse Model, Present Solar (Tungsten Lamps)

TTV, °K	RTV = 0.95 TL = 310°K	RTV = 0.75 TL = 310°K	RTV = 0.65 TL = 310°K
250	304.45*	260.46*	256.58*
275	321.44*	283.45*	280.30*
300	340.26*	307.05*	304.41
325	360.45*	331.05	328.77
350	381.69*	355.32	353.30
375	403.72*	379.76	377.94
400	426.34*	404.32	402.67
425	449.43*	428.97	427.46
450	472.85*	453.69	452.29

TTV, °K	RTV = 0.45 TL = 310°K	RTV = 0.25 TL = 310°K	RTV = 0.05 TL = 310°K
250	252.93*	251.20	250.19
275	277.34	275.95	275.15
300	301.94	300.79	300.12
325	326.66	325.68	325.11
350	351.45	350.59	350.09
375	376.30	375.53	375.08
400	401.18	400.48	400.08
425	426.08	425.44	425.07
450	451.01	450.41	450.06

*Signal below minimum detectable signal

Table 4. Temperature Error Caused in Mark I Chamber by IR Noise Sources, Specular Model, Present Solar (Tungsten Lamps)

TTV, °K	RTV = 0.95 TL = 310°K	RTV = 0.75 TL = 310°K	RTV = 0.65 TL = 310°K
250	498.95*	315.60*	294.31*
275	506.84*	331.51*	312.40*
300	516.99*	349.60*	332.17
325	528.82*	368.72	353.17
350	542.20*	389.27	375.09
375	557.01*	410.71	397.66
400	573.08*	432.83	420.74
425	590.26*	455.51	444.19
450	608.41*	478.58	467.93

TTV, °K	RTV = 0.45 TL = 310°K	RTV = 0.25 TL = 310°K	RTV = 0.05 TL = 310°K
250	271.59*	259.32	251.51
275	292.73	282.51	276.20
300	314.98	306.27	301.00
325	337 93	330.38	325.85
350	361.40	354.72	350.75
375	385.24	379.22	375.67
400	409.32	403.83	400.60
425	433.59	428.52	425.56
450	458.00	453.27	450.52

*Signal below minimum detectable signal

of the lamp collimating tube. Tables 5 and 6 correspond to the IR camera performance in the Mark I chamber with the planned xenon lamp solar simulator. This xenon lamp solar simulator will horizontally irradiate the test object. The flanges holding the quartz lenses for this solar simulator will be water cooled. Thus, the calculations corresponding to Tables 3, 4, 5, and 6 are for water-cooled quartz lenses which will yield a temperature of about 310°K (100°F).

Similar to Table 3, it is seen that the primary limit for diffuse surfaces in the Mark I chamber is the minimum detectable signal (Tables 3 and 5). If again a maximum temperature error of 5°K is considered, then the performance of the IR camera in the Mark I chamber for diffuse surfaces is seen to be about the same as the performance in the 12V chamber. This is illustrated in Fig. 10 where it is shown that the range of applicability for both solar simulators and for diffuse surfaces is about the same. The applicability of the camera for specular surfaces is seen to be much improved for the planned solar in the Mark I as opposed to the present system. The IR noise sources are greater in the Mark I chamber because of the large area of the highly emitting (0.65 emittance 8 to 14 μ) quartz (310°K) as opposed to the very low emitting (0.05 emittance) collimating mirror in the 12V chamber. Tables 4 and 6 illustrate the

Table 5. Temperature Error Caused in Mark I Chamber by IR Noise Sources, Diffuse Model, New Solar (Xenon Lamps)

TTV, °K	RTV = 0.95 TL = 310°K	RTV = 0.75 TL = 310°K	RTV = 0.65 TL = 310°K
250	313.36*	262.48*	257.89*
275	329.49*	285.14*	281.36*
300	347.51*	308.47*	305.31
325	367.04*	332.27	329.54
350	387.72*	356.39	353.98
375	409.28*	380.72	378.55
400	431.51*	405.20	403.22
425	454.26*	429.79	427.97
450	477.41*	454.46	452.76

TTV, °K	RTV = 0.45 TL = 310°K	RTV = 0.25 TL = 310°K	RTV = 0.05 TL = 310°K
250	253.54*	251.44	250.23
275	277.83	276.15	275.18
300	302.34	300.95	300.15
325	327.00	325.82	325.13
350	351.75	350.71	350.11
375	376.56	375.64	375.10
400	401.42	400.58	400.09
425	426.31	425.53	425.08
450	451.22	450.50	450.08

*Signal below minimum detectable signal

Table 6. Temperature Error Caused in Mark I Chamber by IR Noise Sources, Specular Model, New Solar (Xenon Lamps)

TTV, °K	RTV = 0.95 TL = 310°K	RTV = 0.75 TL = 310°K	RTV = 0.65 TL = 310°K
250	358.81*	273.98*	265.45*
275	371.64*	294.78*	287.57*
300	386.53*	316.71*	310.56
325	403.19*	339.47	334.08
350	421.32*	362.76	357.98
375	440.66*	386.46	382.15
400	460.97*	410.44	406.50
425	482.06*	434.63	430.99
450	502.79*	458.97	455.58

TTV, °K	RTV = 0.45 TL = 310°K	RTV = 0.25 TL = 310°K	RTV = 0.05 TL = 310°K
250	257.07*	252.92	250.46
275	280.69	277.33	275.37
300	304.74	301.93	300.31
325	329.05	326.65	325.26
350	353.55	351.45	350.23
375	378.17	376.29	375.20
400	402.88	401.17	400.19
425	427.65	426.08	425.17
450	452.46	451.00	450.16

*Signal below minimum detectable signal

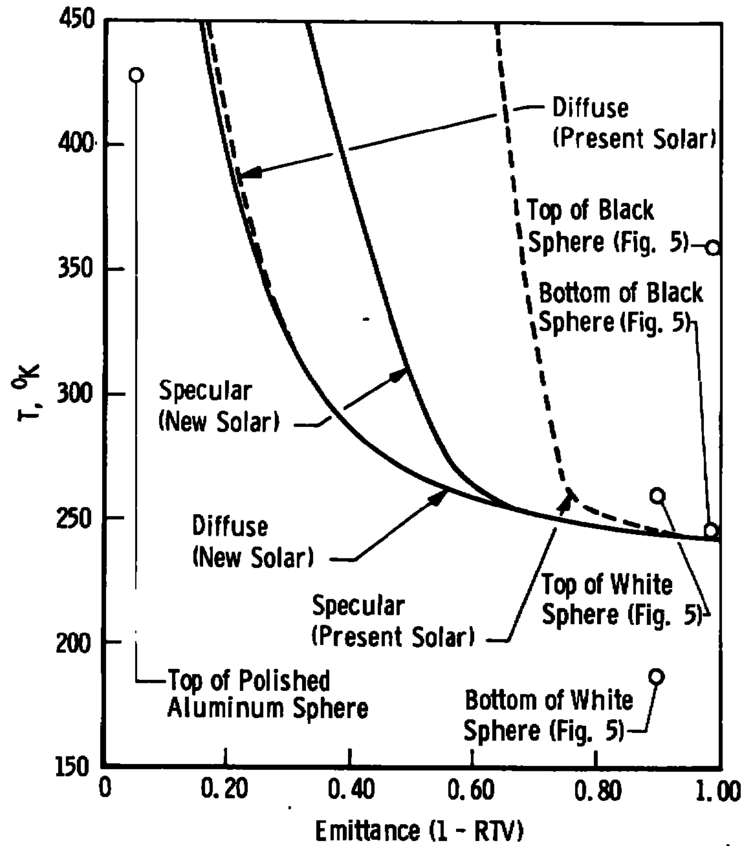

Figure 10. Applicability range of the IR scanning camera in the Mark I chamber for 5° K maximum temperature error.

magnitude of the temperature error for specular surfaces in the Mark I chamber. Although the range of applicability is limited to 5°K error, the camera can still be used to locate test apparatus hotspots for specular surfaces as was illustrated earlier for the 12V chamber. Also indicated in Fig. 10 are the data from Fig. 5 depicting the temperature range of the black painted, white painted, and polished aluminum spheres.

For use of the IR scanning camera in association with either the 12V or Mark I vacuum chambers, it will be necessary to employ an optical material of high IR transmission (8 to 14 μ) as a window in the chamber viewport. Many materials are available, some being relatively inexpensive, such as sodium chloride. Shown in Fig. 11 are several candidate IR window materials (sodium chloride NaCl, potassium bromide KBr, and Cesium bromide CsBr). All these materials are seen to have a transmittance of 0.90 or better in the 8- to 14-μ wavelength region; therefore, the calculations made in this section (Tables 1 through 6 and Figs. 9 and 10) are based on a chamber window transmittance of 0.90.

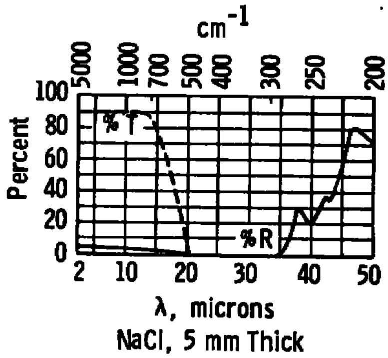

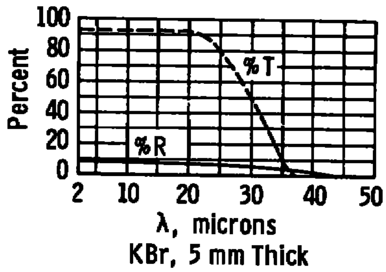

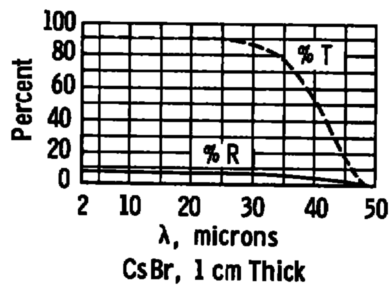

Figure 11. Candidate materials for an IR viewport window in the 12V and Mark I chambers, Ref. 7.

4.0 CALIBRATION AND NECESSARY INPUT DATA

In order to determine absolute temperature from the camera analog signal, it will be necessary to calibrate the IR scanning camera. This will require a determination of the camera analog signal as a function of blackbody flux in the 8- to 14-μ wavelength range or a calibration of the camera in the 2- to 5-μ band with an antisolar filter attached. The flux in either of these wavelength regions can be adjusted by varying the blackbody temperature. Once the analog signal as a function of blackbody temperature has been determined, the calibration can be adjusted to account for the surface emissivity of a test vehicle being different from unity (blackbody emissivity). The calibration can be made at atmospheric pressure inside the chambers

for temperatures above ambient, but a cooled vacuum chamber will be needed for low temperature calibration. It will also be necessary to know or be able to measure the monochromatic directional reflectance (from which the emittance is determined) of the various surface finishes and paints used on a test vehicle. The Beckman IR-4, which operates monochromatically in the 1- to 14-μ range, could be used to make these reflectance measurements. Also, the hemi-ellipsoidal reflectometer, which is operational for room temperature measurements, could also be used to measure the monochromatic directional reflectance.

The calibration will be recorded as an analog signal versus blackbody temperature with f number as a parameter. In order to adjust the camera calibration to account for the IR noise sources in the chamber, the integrating lens and collimating mirror temperatures would be monitored in the 12V chamber and the collimator tube cover temperature would be monitored in the Mark I chamber. Since calibration sources from camera manufacturers are available only in the 16 to 100°C range, it will be necessary to seek or develop other calibration standards outside of this range. It is recommended that a large blackbody (about 6 in. in diameter) be constructed that operates in the range of -50 to 100°C. This could be designed and fabricated very economically from aluminum.

A typical plot of an IR scanning camera calibration taken from Ref. 9 is shown in Fig. 12, where the voltage output from the camera

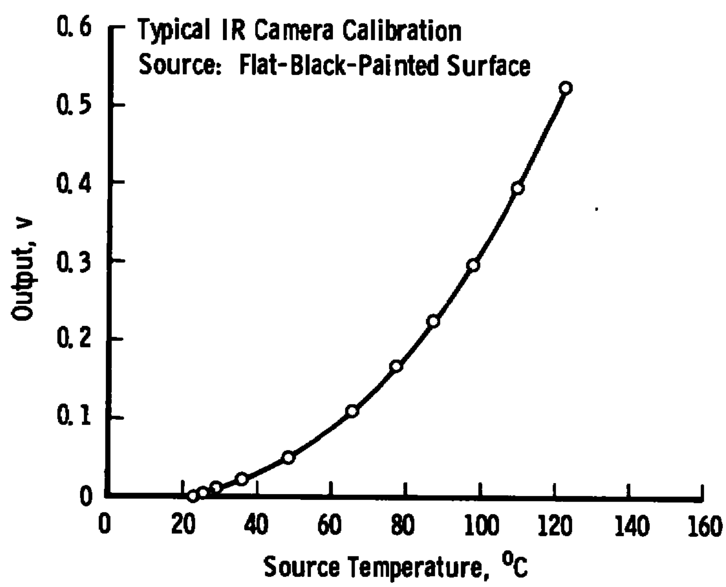

Figure 12. IR scanning camera calibration, Ref. 9.

is plotted as a function of blackbody source temperature. The author of Ref. 8 asserts that repeatability between calibrations was within one percent. Shown in Fig. 13 is a typical calibration (Ref. 4) of the AGA Model 680 camera; the isothermal units are proportional to analog voltage.

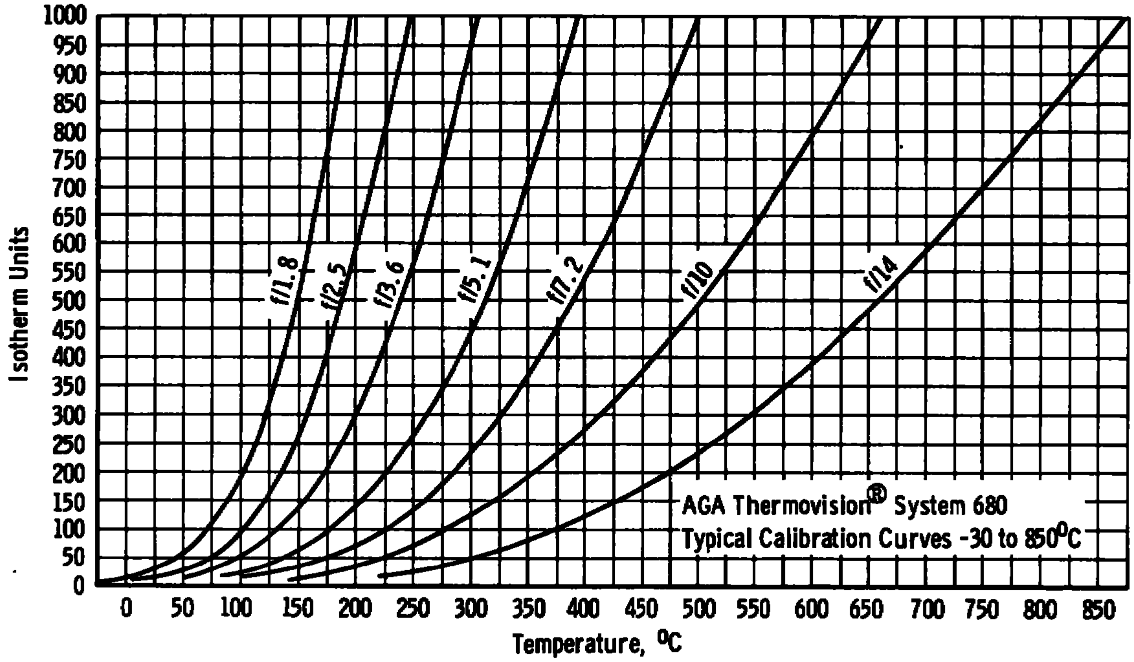

Figure 13. Typical calibration curves (-30°C to 850°C) as a function of f number, Ref. 5.

The scanning camera will require recalibration because of the use of filters such as the antisolar filter and because of use of a view-port window (Refs. 6 and 9) (in this case a CaF_2 window). It is also desirable to check the camera spatial resolution, which requires the use of a calibration blackbody. The blackbody that will be designed can be used for calibration, determination of spatial resolution, and determination of temperature resolution. The spatial and temperature resolution are both quoted by camera manufacturers; however, it will be necessary to check these values and camera calibration periodically.

5.0 DATA COLLECTING AND RECORDING

One of the basic requirements of using the IR scanning camera to obtain temperature maps of test articles is its coupling with a computer. A block diagram for the IR scanning camera data system

is shown in Fig. 14. This diagram indentifies the flow of information and the various components in the system. This data system will allow the acquisition of digital data from a variable speed IR scanning camera whose output is in analog form. By using this system, the field of view shown on the camera monitor can be stored and analyzed in parts or in its entirety. The number of lines per frame may be varied and/or the number of samples per line may be varied. The data system provides a means of looking at the portion of the picture being stored in the computer through a CRT monitor.

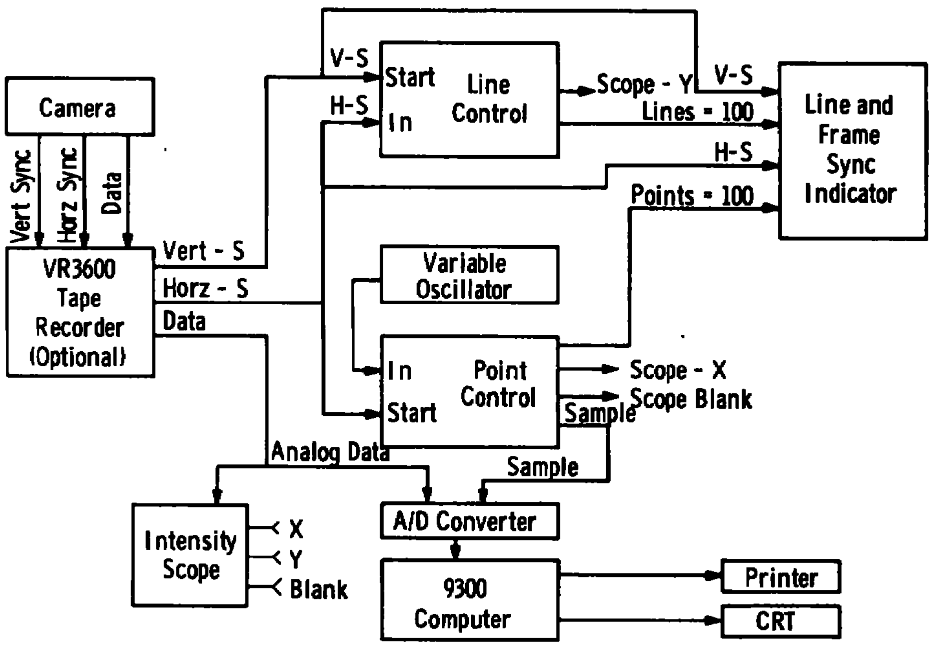

Figure 14. Block diagram of IR scanning camera data system.

The analog signal from the camera may be recorded on a tape recorder (Fig. 14). The tape recorder is required only for high data rates. Data may be recorded at high tape speed from the camera and then replayed at a slower speed into the camera data system. This is done because the data system can only process 100,000 bits of data per second.

The data system has a line control (Fig. 14) which is initiated by the vertical sync pulse. The line control counts the horizontal sync pulses until it reaches the number of lines specified for one frame. Then it sends out a pulse to indicate that the number of lines constituting one frame has been attained. The number of lines is converted

to an analog value as it is counted so that this analog voltage can control the Y deflection on an oscilloscope. The number of lines per frame indicated on the diagram is 100; however, the number can be programmed by thumbwheel switches.

Included in the data system is a variable oscillator (Fig. 14) which is manually set to operate at some multiple horizontal sync frequency. This multiple will be equal to the number of points desired per line (typically 100).

The point control (Fig. 14) has its operation initiated by the horizontal pulse signal. The point control counts pulses from the variable oscillator (or camera chopper) until it reaches the proper number of points for one line. This number can be set with thumbwheel switches. When this preset number is reached, it sends out a pulse. In addition, it sends out another pulse to indicate when each sample should be taken. Like the line control, it generates an analog signal; this signal controls the X deflection of a CRT beam. It also sends out a signal for blanking the CRT beam while it is retracing.

The line and frame sync indicator (Fig. 14) compares the timing of the sync pulses with the count completion pulses to ensure that the proper numbers of points are being produced between horizontal sync pulses and the correct numbers of lines are being generated between vertical sync pulses.

The A/D converter shown in Fig. 14 is used to transform the analog signal into digital information. The analog data are fed continually into the converter and are digitized only when a valid data point appears. The sample pulse occurs simultaneously with the valid data point and activates the converter. The digitized data are then stored in the SDS 9300 computer. The scope (Fig. 14) is an optional feature which will allow viewing the picture which is actually being stored by the computer.

This data system will allow the computer to determine a temperature map of the test article in the vacuum chamber. From this, qualitative information may be obtained such as the location of hotspots. Also, the computer will permit the rapid acquisition of quantitative information such as the radiative flux and temperature maps. The radiative flux or surface temperature along any (camera) line in the field of view can be graphed as a function of lateral position; this graph can be displayed on the CRT, and a hard copy may be produced.

Thus, the data system will permit both digital and graphic representation of the camera data. The data system will also permit the camera information to be processed either in a coarse mesh or in a fine mesh depending upon test requirements.

6.0 CONCLUSIONS AND RECOMMENDATIONS

The range of applicability of an IR camera can be seen in light of the results presented in Section 3.0. Generally, this type camera would appear to have a good range of application for 12V testing, but appears to have a more restricted range of usefulness in the Mark I chamber with respect to quantitative information retrieval (temperature and flux levels) as long as the present solar simulator remains in use. The camera would appear to be quite useful in both chambers for qualitative information (locating hotspots). The range of camera usefulness for measuring temperatures with 5°K accuracy or better was presented in Figs. 9 and 10 for the 12V and Mark I chambers, respectively.

There is need to make a series of measurements under controlled operating conditions in the 12V chamber in order to validate the studies reported herein. This could be carried out using the currently available camera with the addition of a suitable solar filter.

REFERENCES

1. Thomann, H. and Frisk, B. "Measurement of Heat Transfer with an Infrared Camera." International Journal of Heat and Mass Transfer, Vol. 11, 1968, pp. 819-826.

2. Compton, D. L. "Use of an Infrared-Imaging Camera to Obtain Convective Heating Distributions." AIAA Journal, Vol. 10, No. 8, August 1972, pp. 1130-1132.

3. Lorentz, A. Personal communication during visit to AEDC, Arnold Air Force Station, Tennessee, November 8, 1973.

4. "AGA Thermovision System 680/102B Operating Manual." AGA Aktrebolog Infrared Instruments Dept., Liedingo, Sweden, Publication 556.053.

5. Warner, R. M. "Description and Performance of the 8-Ft Diameter Solar Simulator System at AEDC." AEDC-TR-67-219 (AD821819), October 1967.

6. McCarthy, D. E. "The Reflection and Transmission of Infrared Materials: I, Spectra From 2-50 Microns." Applied Optics, Vol. 2, No. 6, June 1963, p. 591.

7. Norman, C. F. "Design and Initial Operation of a Large Low-Cost Solar Simulator Using Tungsten Lamps with Collimating Tubes." AEDC-TR-69-198 (AD863025), December 1969.

8. Compton, D. L. "Convective Heating Measurements by Means of an Infrared Camera." NASA TMX-2507, Space Shuttle Aerothermodynamics Technology Conference, Vol. II - Heating, February 1972, pp. 645-660.

9. Wolfe, W. L., Editor Handbook of Military Infrared Technology. Office of Navel Research, Department of the Navy, Washington, D. C., 1965.

APPENDIX A
LENS CHARACTERISTICS

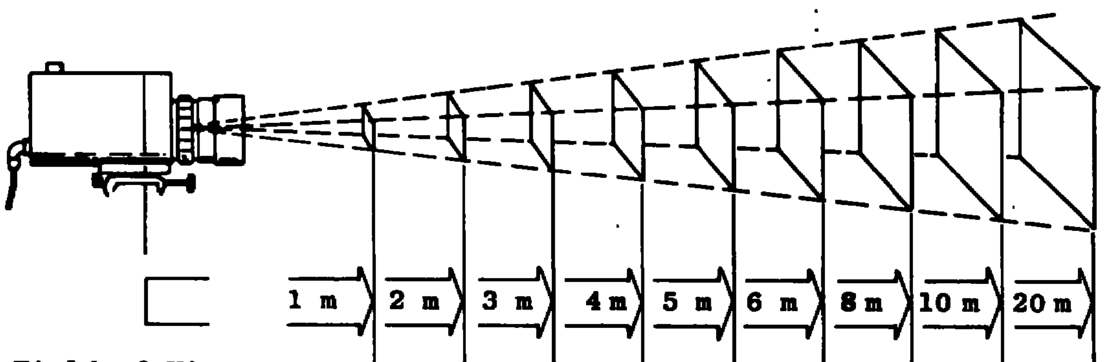

Field of View, m									
10-deg Lens	0.13	0.30	0.47	0.65	0.83	1.0	1.4	1.7	3.5
25-deg Lens	0.40	0.85	1.30	1.73	2.18	2.6	3.5	4.4	8.9
45-deg Lens	0.77	1.61	2.44	3.26	4.08	4.9	6.6	8.2	16.5
Depth of Focus*									
10-deg Lens	0.04	0.2	0.5	0.8	1.3	2	3.4	5.5	22
25-deg Lens	0.3	1.4	3.1	5.6	9	13	23	35	--
45-deg Lens	1.1	4.6	10.5	19	30	43	--	--	--

*Depth of focus at these distances is shown for aperture setting f/1.8; smaller apertures (larger f/stops) give greater depths of focus.

Figure A-1. Lens characteristics.

APPENDIX B
BASIC EQUATIONS

The derivation of the equations, from which the results shown in Tables 1 through 6 were computed, is presented and discussed in the following. In the 12V chamber, the camera detector will respond to the sum of three radiation signals: (1) the radiation emitted by the quartz integrating lens which after reflection from the collimating mirror and test vehicle is incident upon the camera, (2) the radiation emitted by the collimating mirror which after reflection from the test vehicle is incident upon the camera, and (3) the radiation which is emitted by the test vehicle and is incident upon the camera. The derivations will be presented for both a specular test vehicle and a diffuse test vehicle.

Since the various emitting surfaces are located at relatively large distances from each other, all of the areas will be treated as differential area elements. The area of the integrating lens will be designated by dA_L, the area of the collimating mirror by dA_M, and the area element dA_{TV}, is an element of area of the test vehicle projected normal to the direction in which the IR scanning camera is focused. The temperatures of these same three area elements will be designated by T_L, T_M, and T_{TV}.

LENS IR NOISE

The monochromatic radiative power emitted by the integrating lens and incident upon the collimating mirror is given by

$$dP_\lambda = \frac{\epsilon_{L,\lambda}\ e_{bb,\lambda}(T_L)\ \cos\ \beta_1\ \cos\ \beta_2\ dA_L\ dA_M}{\pi r^2} \qquad \text{(B-1)}$$

where $\epsilon_{L,\lambda}$ is the lens monochromatic emissivity, $e_{bb,\lambda}$ is Plank's blackbody function, r is the distance from the center of the integrating lens to the center of the collimating mirror, and β_1 (20 deg) and β_2 (25 deg) are the angles, respectively, between the normals to dA_L and dA_M and the vector r connecting the centers of these two areas. The radiative power emitted by the lens and incident upon the mirror in the 8- to 14-μ band is given by

$$dP = \frac{\cos\ \beta_1\ \cos\ \beta_2\ dA_L\ dA_M}{r^2} \int_{8\ \mu}^{14\ \mu} \frac{\epsilon_{L,\lambda}\ e_{bb,\lambda}\ (T_L)\ d\lambda}{\pi} \qquad \text{(B-2)}$$

For the sake of simplicity it will be assumed that the emissivities and reflectivities are essentially constant in the 8- to 14-μ range. The power reflected from the collimating mirror (mirror reflectivity = ρ_M) is given by

$$dP_{LM} = \frac{\rho_M \ \epsilon_L \cos \beta_1 \cos \beta_2 \ dA_M \ dA_L}{r^2} \int_{8\,\mu}^{14\,\mu} \frac{e_{bb,\lambda} \ (T_L) \ d\lambda}{\pi} \tag{B-3}$$

The collimated flux reflected from the mirror may be written as

$$F_o = \frac{dP_{LM}}{dA_M} = \frac{\rho_M \ \epsilon_L \cos \beta_1 \cos \beta_2 \ dA_L}{r^2} \int_{8\,\mu}^{14\,\mu} \frac{e_{bb,\lambda} \ (T_L) \ d\lambda}{\pi} \tag{B-4}$$

DIFFUSE TEST VEHICLE

The flux incident upon an area element of the test vehicle is

$$F = F_o \cos \theta^* \tag{B-5}$$

where θ^* is the angle between the normal to the area element and the incident collimated radiation. The diffusely reflected intensity from the test vehicle is the diffusely reflected flux divided by

$$I_r = \frac{\rho_{TV} \ F_o \cos \theta^*}{\pi} \tag{B-6}$$

In order to estimate the maximum IR noise intensity resulting from the integrating lens, let cos θ^* = 1. Thus, the power reflected from the test vehicle to the camera is

$$dP_C = \frac{I_r \ dA_{TV} \ dA_C}{f^2} \tag{B-7}$$

where f is the camera focal length and dA_C is the camera collecting area. The cosines do not appear in the above expression because the

camera acts as a focused system. Thus, the final expression for the flux emitted by the integrating lens and incident upon the camera is

$$\left.\frac{dP_C}{dA_C}\right)_{\text{LENS}} = \frac{\rho_{TV}\ \rho_M\ \epsilon_L\ \cos\ \beta_1\ \cos\ \beta_2}{\pi}\ \frac{dA_L}{r^2}\ \frac{dA_{TV}}{f^2}\int_{8\ \mu}^{14\ \mu}\frac{e_{bb,\lambda}(T_L)\ d\lambda}{\pi} \tag{B-8}$$

SPECULAR TEST VEHICLE

For a specular test vehicle the IR noise generated by the lens will only affect the camera when it is incident upon the test vehicle at the specular angle. If the model is examined by the camera at two axial chamber locations, then the IR noise from the lens may be totally illuminated. Thus, for a specular test vehicle the IR noise generated by the integrating lens is considered negligible.

MIRROR IR NOISE

The flux emitted by the mirror and incident upon the test vehicle is

$$\frac{dP_M}{dA_{TV}} = \frac{(1 - \rho_M)\ dA_M}{R^2}\int_{8\ \mu}^{14\ \mu}\frac{e_{bb,\lambda}\ (T_M)\ d\lambda}{\pi} \tag{B-9}$$

The diffusely reflected intensity is the diffusely reflected flux divided by π.

$$I_{Mr} = \frac{\rho_{TV}\ (1 - \rho_M)\ dA_M}{\pi R^2}\int_{8\ \mu}^{14\ \mu}\frac{e_{bb,\lambda}(T_M)\ d\lambda}{\pi} \tag{B-10}$$

The power reflected from dA_{TV} to the camera is

$$dP_{MC} = \frac{I_{Mr}\ dA_{TV}\ dA_C}{f^2} \tag{B-11}$$

or the flux incident upon the camera may be expressed by

$$\left.\frac{dP_{MC}}{dA_C}\right)_{MIRROR} = \frac{\rho_{TV}\ (1 - \rho_M)}{\pi} \left(\frac{dA_M}{R^2}\right)\left(\frac{dA_{TV}}{f^2}\right)\int_{8\ \mu}^{14\ \mu} \frac{e_{bb,\lambda}(T_M)\ d\lambda}{\pi} \tag{B-12}$$

The monochromatic intensity emitted by the mirror is given by

$$I_M = \frac{(1 - \rho_M)\ e_{bb,\lambda}\ (T_M)}{\pi} \tag{B-13}$$

The solid angle dA_C/f^2 viewed by the camera is equal to, as shown in Fig. B-1, the incident solid angle dA_3/R^2. The monochromatic power leaving dA_3 (which is a portion of the area of the collimating mirror) and incident upon the test vehicle is

$$dP_{\lambda,M} = I_M \cos\gamma\ d\omega\ dA_{TV} \tag{B-14}$$

or

$$dP_{\lambda,M} = I_M \cos\gamma\ \frac{dA_3}{R^2}\ dA_{TV} \tag{B-15}$$

In order to estimate the maximum noise let $\cos\gamma = 1$; therefore, the noise in the 8- to 14-μ wavelength region incident upon dA_{TV} becomes

$$dP_M = (1 - \rho_M)\ \frac{dA_3}{R^2}\ dA_{TV} \int_{8\ \mu}^{14\ \mu} \frac{e_{bb,\lambda}\ (T_M)\ d\lambda}{\pi} \tag{B-16}$$

The intensity reflected from the test vehicle differential area element toward the camera is $\rho_{TV}\ I_M$. Substituting $dA_3/R^2 = dA_C/f^2$, the flux emitted by the mirror which is incident upon the camera after reflection from a specular test vehicle becomes

$$\left.\frac{dP_M}{dA_C}\right)_{MIRROR} = (1 - \rho_M)\ \rho_{TV}\ \frac{dA_{TV}}{f^2} \int_{8\ \mu}^{14\ \mu} \frac{e_{bb,\lambda}(T_M)\ d\lambda}{\pi} \tag{B-17}$$

TEST VEHICLE SIGNAL

The radiative flux emitted from the test vehicle and incident on the camera is

$$\left.\frac{dP_{TV}}{dA_C}\right)_{\substack{\text{TEST}\\ \text{VEHICLE}}} = \frac{(1 - \rho_{TV})\ dA_{TV}}{f^2} \int_{8\ \mu}^{14\ \mu} \frac{e_{bb,\lambda}\ (T_{TV})\ d\lambda}{\pi} \tag{B-18}$$

The above equations are an outline of those used in obtaining the results shown in Tables 1 through 6. The calculations for the Mark I chamber did not include any noise contributions from an integrating lens; rather, the energy emitted by the quartz lamp envelopes was treated the same as the mirror noise term in the 12V chamber except the mirror emissivity was replaced by the quartz envelope emissivity.

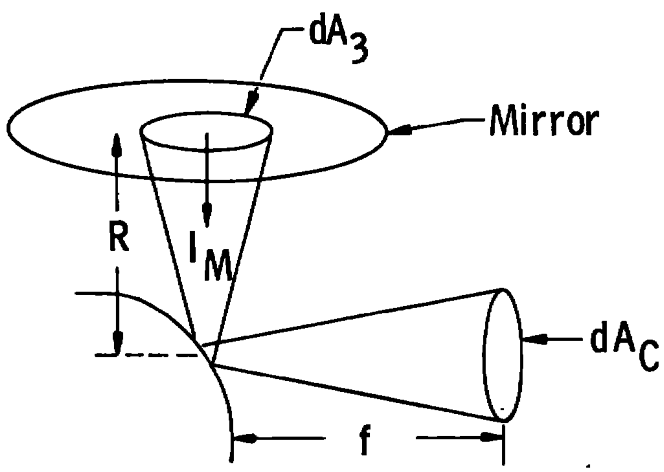

Figure B-1. Specular reflection sketch.